

# Reddy: An open-source toolbox for analyzing eddy-covariance measurements in heterogeneous environments

Laura Mack<sup>1,\*</sup>, Norbert Pirk<sup>1</sup>

*<sup>1</sup>: Department of Geosciences, University of Oslo, Oslo, Norway*

*\*Correspondence: laura.mack@geo.uio.no*

## Abstract

Land-atmosphere exchange processes are determined by turbulent fluxes, which can be derived from eddy-covariance measurements. This method was established to quantify ecosystem-scale vertical atmosphere-vegetation exchange processes, but is also used to validate atmospheric turbulence theories with the ultimate aim to improve the representation of turbulence in numerical models. While the focus has long been on turbulence over idealized, homogeneous and flat surfaces, recent scientific developments are shifting towards investigating turbulent exchange processes in complex heterogeneous environments under non-idealized conditions, which pose particular challenges, e.g. advective fluxes between different surface types or non-stationarity of nighttime turbulence. This requires to rethink standard post-processing routines for determining turbulent fluxes from the high-frequency sonic and gas analyzer measurements. Here, we introduce the open-source R-package 'Reddy', which provides modular-built functions for post-processing, analysis and visualization of eddy-covariance measurements, including investigating spectra, coherent structures, anisotropy, flux footprints and surface energy balance closure. The 'Reddy' package is accompanied by a detailed documentation and a set of jupyter notebooks introducing new users hands-on to eddy-covariance data analysis. We showcase 'Reddy' based on measurements from three different sites in Norway: A case study during strong stratification over alpine tundra, for determining suitable averaging times during ice-cover transition at a boreal lake, and for fitting flux-variance relations for a permafrost peatland. 'Reddy' serves as extension of previously developed software packages, paving the way towards holistic turbulence data analysis in heterogeneous real-world environments.

## 1 Introduction

Turbulent fluxes are the main driver of land-atmosphere and vegetation-atmosphere interactions (e.g. Baldocchi, 2003, 2020), and the standard technique for measuring them is eddy-covariance (e.g. Aubinet et al., 2012). Strictly speaking, however, eddy-covariance is only the method used to calculate fluxes from high-frequency sonic and gas analyzer measurements of three-dimensional wind speed, temperature and trace gases, which enable in-depth analysis of turbulence characteristics.

To derive turbulent fluxes of sensible heat, latent heat, carbon dioxide or further trace gases from the high-frequency measurements, several software packages have been developed that offer a range of post-processing options for deriving vertical exchange between vegetation and atmosphere, most notably EddyPro (LI-COR Biosciences, 2017). These software packages are well-tested and robust, leading to a high

agreement of the derived turbulent fluxes (Mauder et al., 2008; Fratini and Mauder, 2014; Mammarella et al., 2016), and have served as tools to generate regional or global flux products, e.g. within FLUXNET (Pastorello et al., 2020) or the Integrated Carbon Observation System (ICOS).

However, recent scientific developments are moving towards studying turbulent fluxes in more complex heterogeneous environments (e.g. Rotach and Holtslag, 2025), requiring a rethinking of common post-processing routines, which were typically developed for homogeneous flat terrain under idealized well-mixed turbulence conditions. For example, in highly heterogeneous environments, horizontal gradients at the interface of different surface types, e.g. between lake and forest or snow patches, can introduce lateral advective fluxes. Under wintertime stable conditions, turbulence can become intermittent and non-stationary influenced by non-local wave transport (e.g. Mahrt, 2014), leading to notable low-frequency contributions to fluxes (e.g. Sievers et al., 2015; Pirk et al., 2017). In these cases, the standard post-processing procedure to derive vertical fluxes based on 30 minutes averaging, might not be sufficient. Instead, post-processing and analysis steps of turbulence characteristics have to be linked in a re-evaluation cycle in order to adapt the post-processing methods to the specific site and environmental conditions. In this regard, it is also desirable that not only post-processing but also standard analysis routines are available in open-source software. Accordingly, software packages for selected applications of eddy-covariance data analysis have been developed, e.g. 'REddyProc' focusing on gap-filling and flux partitioning (Wutzler et al., 2018) or 'bigleaf' for deriving physiological ecosystem properties from eddy-covariance data (Knauer et al., 2018).

Here, we expand on these recent advancements by introducing the open-source software package 'Reddy', which is built in a modular fashion enabling customized post-processing routines as well as performing several analysis steps, that help to determine suitable averaging times by characterizing turbulence properties through the combination of analyzing spectra, coherent structures, flux footprints and turbulence topology. Additionally, 'Reddy' also provides functions to treat output from numerical weather prediction systems, analyze it and use eddy-covariance measurements for model verification and development (Mack et al., 2025b).

We first explain the package structure and the main analysis steps, including post-processing, calculation of turbulence diagnostics, and visualization of the results. Subsequently, we showcase parts of the package functionality for dual-site measurements in the alpine valley Finse (Southern Norway), for a measurement campaign at the boreal lake Langtjern (Southern Norway), and the permafrost peatland Iškoras (Northern Norway). These sites are characterized by heterogeneous and changing surface conditions, meaning that analyzing turbulence characteristics requires a modular, step-by-step approach, which is precisely what 'Reddy' was specifically developed for.

## 2 Package Description

The 'Reddy' package provides functions for both raw data processing and standardized analysis of the post-processed eddy-covariance data, as showcased in Fig. 2.1 and described in the following.

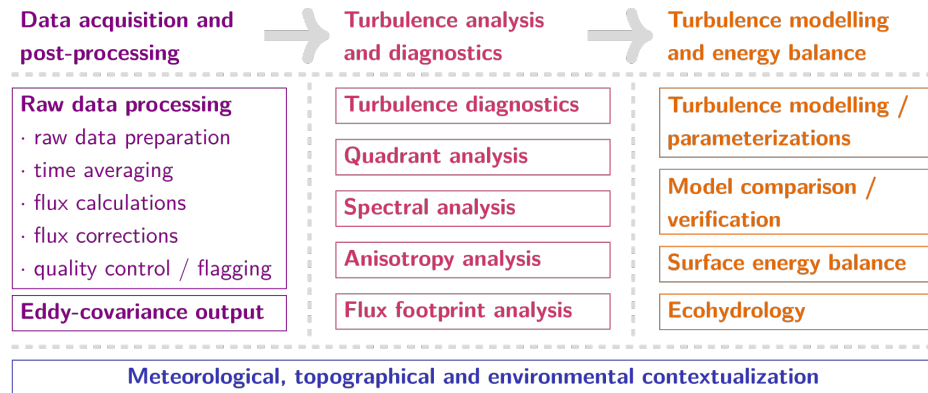


Figure 2.1: Components and workflow from eddy-covariance raw data to application in 'Reddy'.

## 2.1 Data processing

The raw data processing of the high-frequency eddy-covariance data in 'Reddy' follows the usual four-step procedure (e.g. Fratini and Mauder, 2014):

- **step1: raw data preparation:** The raw data is despiked by using pre-defined thresholds (plausibility limits), skewness and kurtosis thresholds, and the median deviation test (Mauder et al., 2013). Additionally, variable conversions, e.g. from speed of sound to sonic temperature, and unit conversions are performed. The separation between gas analyzer and sonic can be corrected for with a lag-time correction applying the maximum cross-correlation method.
- **step2: tilt correction, time averaging and flux calculation:** Tilt correction is performed by rotating the axes of the three-dimensional wind measurements. 'Reddy' provides two methods for this: (1) double rotation, to rotate the wind into a streamline-following natural coordinate system per chosen averaging time window, and (2) planar fit rotation, to rotate the wind into a mean-streamline plane (Wilczak et al., 2001). Double-rotation is recommended for flat and homogeneous terrain as well for sites with changing surface properties, e.g. during snow melt-out or growing season, while planar fit is the preferred method in complex sloped terrain. Afterwards, the means, variances and covariances of the desired quantities are calculated using block or rolling average and the covariances are transformed to fluxes. To accelerate these calculations, 'Rcpp' is used which facilitates a seamless integration of R and C++ (Eddelbuettel, 2013). The aim of this step is to separate the active eddy turbulent transport from deterministic larger-scale motions, and thus depends strongly on the studied site (Moncrieff et al., 2005), so that re-iterating post-processing and analysis steps (detailed in sec. 2.3) is necessary.
- **step3: flux corrections:** Depending on used instruments and conditions, the fluxes require specific corrections. To convert from buoyancy flux (based on sonic temperature) to sensible heat flux, SND correction (Schotanus et al., 1983) is applied, which usually includes the cross-wind correction (Liu et al., 2001). For the gas fluxes, volume-related quantities have to be converted to mass-related quantities by applying a density correction, which is achieved with the WPL correction (usually for open-path systems) (Webb et al., 1980) or with the adjustments of Ibrom et al. (2007) to account for de-synchronized dilution of water vapor and CO<sub>2</sub> flux (usually used for closed-path systems). The

limited frequency response of the measurement system acts as low-pass filter and resulting spectral loss needs to be corrected for (Massmann, 2000). However, when a lag-time correction with maximum cross-correlation is applied (in step 1) it corrects for both sensor separation and limited frequency response, resulting in an underestimation of high-frequency contributions, which can be accounted for with a transfer function (Peltola et al., 2021a).

- **step4: quality control and flagging:** The quality control follows the flagging system introduced by Mauder et al. (2013) applying a distortion flag, a vertical velocity flag, a stationarity flag (Foken and Wichura, 1996) and an integral turbulence characteristics flag that tests the agreement with similarity scalings from Panofsky and Dutton (1984). In this 0-1-2 system, the flags take the values of 0 (good data quality), 1 (acceptable data quality) and 2 (recommended to discard). Additional quality control diagnostics provided are number of spikes and amplitude resolution.

In 'Reddy', all the described methods are implemented as separate functions, which are ultimately combined in one post-processing routine, but can also be integrated by the user in an own customized workflow.

## 2.2 Calculation of turbulence diagnostics

From the post-processed data, several standard turbulence diagnostics, such as friction velocity, turbulent kinetic energy, turbulence intensity, directional shear angle, Obukhov length, stability parameter and flux Richardson number can be calculated in 'Reddy'. Intermittency can be characterized with the flux intermittency indicator from Mahrt (1998). The turbulence topology can be investigated by calculating the velocity aspect ratio (e.g. Mahrt, 2011) or by performing an invariant analysis of the full Reynolds stress tensor, which also takes the shear stresses into account.

If additionally to the eddy-covariance measurements also (slow-sampled) vertically distributed temperature and/or wind speed measurements are available that allow the derivation of vertical gradients, further bulk diagnostics can be calculated, e.g. eddy diffusivities, Prandtl number, bulk Richardson number, Ozmidov scale (Ozmidov, 1965) and decoupling metric (Peltola et al., 2021b). Also diagnostics for Ekman layer depth and boundary-layer height (Nieuwstadt, 1981) are available.

'Reddy' allows to calculate different topographical and surface characteristics. Based on a given digital elevation model, the topographic position index (TPI), the deviation from mean elevation (DEV), and the slope-based direction-dependent terrain parameter Sx (e.g. Winstral et al., 2017) can be estimated. Surface roughness length can be estimated based on friction velocity using the relation from Charnock (1955).

For meteorological contextualization, standard quantities based on auxiliary measurements can be consulted, e.g., clear-sky index (Marty and Philipona, 2000; Lehner et al., 2019), vapor pressure deficit, saturation vapor pressure and several unit conversions, e.g. of different humidity measures, can be performed. The calculated latent heat flux can be transformed to evaporation and in combination with the sensible heat flux, Bowen ratio and evaporative fraction can be calculated to perform a ecohydrological characterization of the studied site.

## 2.3 Data analysis and visualization

The quality-controlled and post-processed data can be used for several applications, both based on the high-frequency data and the averaged output.

- **spectral analysis:** 'Reddy' provides several functions to calculate and visualize spectra based on the high-frequency measurements. The common Fast Fourier Transform (FFT) spectrum can be calculated and smoothed to compare it with theoretically expected spectral slopes, e.g. to analyze kinetic and potential energy dissipation. Wavenumber spectra can be calculated using FFT and discrete cosine transform (DCT), which is commonly applied to two- or three-dimensional model fields to derive the effective model resolution or compare spectral characteristics between observations and model (e.g. Mack et al., 2025b). To characterize flux contributions on different time scales, multiresolution decomposition (MRD) (Vickers and Mahrt, 2003) can be consulted, which utilizes Haar wavelets. Several MRDs can be combined to a composite MRD, which is a common tool to determine a suitable averaging time for calculating fluxes and turbulence intensities (e.g. Stiperski and Calaf, 2018). Based on both single and composite MRDs, a recommendation for a suitable averaging time can be requested, which applies the algorithm from Vickers and Mahrt (2003) and returns the first zero-crossing (starting from small timescales) after an identified turbulence peak, corresponding to a co-spectral gap separating turbulent and submeso-scale motions. Another way to analyze spectral contributions are ogives, i.e. cumulative distribution functions. While they do not contain different information than the spectra, they appear smoother due to the integration and allow to determine the averaging time based on the convergence rate in an objective numerical way (Sievers et al., 2015).
- **quadrant analysis:** Quadrant analysis is a commonly used tool to analyze coherent structures and their flux contributions based on the high-frequency measurements. 'Reddy' provides the option to visualize a normalized scatter plot indicating the number and flux contributions of the four quadrants for different hyperbolic hole size (i.e. intensities) and to derive simple measures for flow organization, such as ejection-sweep ratio, exuberance (Shaw et al., 1983) or organization ratio (Mack et al., 2024).
- **structure functions:** Structure functions of different orders can be calculated (e.g. van de Water and Herweijer, 1999) as well as two-point correlations (e.g. Ganapathisubramani et al., 2005).
- **anisotropy analysis and barycentric map:** Based on the invariant analysis of the Reynolds stress tensor, the calculated eigenvalues indicate characteristics of turbulence topology and the eigenvectors of the spatial orientation of eddies. The derived anisotropy allows to visualize these properties in a barycentric map (Banerjee et al., 2007), which reveals different anisotropy limiting states.
- **flux footprint:** The flux footprint, i.e. the area where the surface flux originates from, can be estimated based on the post-processed averaged eddy-covariance measurements. In 'Reddy', the analytical flux footprint model from Kormann and Meixner (2001) with the parameters according to Neftel et al. (2008), and the parameterized version of a Lagrangian stochastic model from Kljun et al. (2015) are available. For both, the cross wind-integrated flux footprint (1D flux footprint) and the contours (2D flux footprint) can be calculated, and afterwards geo-localized to be plotted on terrain maps. For a time series of post-processed averaged eddy-covariance measurements, the flux footprint climatology can be calculated for both footprint models.
- **surface energy balance:** If additional to the flux measurements also radiometer measurements are available, the surface energy balance can be studied by calculating and visualizing the closure ratio and the residual flux (e.g. Stoy et al., 2013).

- **model evaluation tools and similarity scalings:** As eddy-covariance data is often used to study and improve turbulence parameterizations in numerical weather prediction or climate models, 'Reddy' also provides some basic tools to study similarity relations for both flux-variance and flux-profile relations, calculate dimensionless shear and temperature gradients and derive theoretical vertical wind and eddy diffusivity profiles. Further auxiliary functions are available to automatize analyzing stability dependence. Standard functions to make numerical model output comparable with measurements are e.g. the conversion of the used vertical model coordinate and the deaccumulation of fluxes (Mack et al., 2025b).

## 2.4 Manual and Documentation

The 'Reddy'-package is in line with the standards from R-CRAN (Comprehensive R Archive Network) and utilizes the 'roxygen2' package for standardized in-code comments to create a detailed PDF manual. This manual contains a detailed description of all functions, their inputs and outputs, accompanied by examples and automatized testing procedures. Additionally, a 'bookdown'-generated GitHub-page ([https://noctiluc3nt.github.io/ec\\_analyze/](https://noctiluc3nt.github.io/ec_analyze/)) showcases and explains the 'Reddy'-package grouped by topics (detailed in sec. 3.4).

## 3 Applications

We showcase parts of the 'Reddy'-package based on eddy-covariance measurements from three different locations in Norway (Fig. 3.1a). Finse (60.11°N, 7.53°E, 1200 m a.s.l.) is an alpine tundra site on the Hardangervidda mountain plateau in Southern Norway. Here, we use measurements from two neighboring sites (distance of 610 m) both equipped with a sonic (CSAT3, Campbell Scientific) and a closed-path gas analyzer for H<sub>2</sub>O and CO<sub>2</sub> (Li-7200, LiCor), as well as slow-sampled auxiliary measurements described in Pirk et al. (2023) and Mack et al. (2024). We investigate a two-day case study during clear-sky conditions (17.03.-18.03.2018) focusing on using 'Reddy' for calculating turbulent diagnostics and surface energy balance closure.

Additionally, we use data from a measurement campaign (12.04.2024-24.06.2024) with a sonic (CSAT3, Campbell Scientific) and an open-path gas analyzer for H<sub>2</sub>O and CO<sub>2</sub> (Li-7500, LiCor) at lake Langtjern (60.37°N, 9.73°E, 517 m a.s.l.) in Southern Norway. This lake is home to a water and climate monitoring station studying the exchange of terrestrial carbon at this lake-forest-atmosphere interface (e.g. Clayer et al., 2021; de Wit et al., 2024). While carbon concentration measurements are routinely performed along a vertical profile through the lake, eddy-covariance measurements are usually not available. The measurement period encompasses the transition between ice-covered and ice-free conditions and we use 'Reddy' to investigate turbulence spectra before and after ice-cover transition.

Lastly, we use two years (2019-2020) of continuous measurements with a sonic (CSAT3, Campbell Scientific) and two gas analyzers (closed-path Li-7200 for H<sub>2</sub>O and CO<sub>2</sub>, and Li-7700 for CH<sub>4</sub>, LiCor) from Iškoras (69.34°N, 25.30°E, 380 m a.s.l.), a permafrost peatland site in Northern Norway (Pirk et al., 2024), to analyze flux-variance relations of trace gases with the help of 'Reddy'.

The data is processed with the 'Reddy' function `ECprocessing()` by applying despiking (`despiking()`), double rotation (`rotate_double()`), SND and WPL correction (`SNDcorrection()`, `WPLcorrection()`),

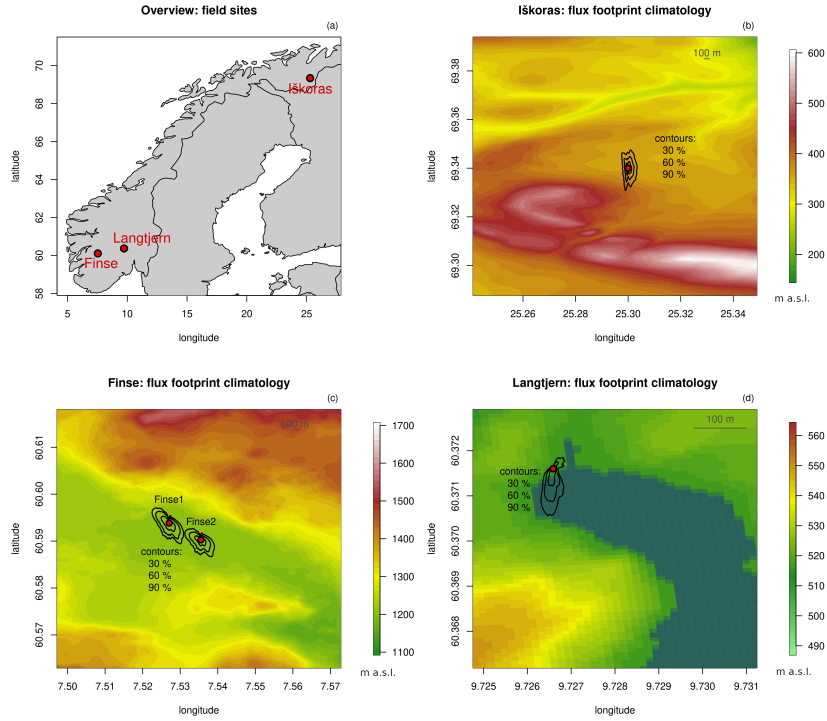


Figure 3.1: Overview of the studied field sites and their flux footprint climatologies: (a) Site locations, (b) Iškoras (used time period: 2019-2020), (c) Finse (used time period: 02/2018-01/2019), (d) Langtjern (during the measurement campaign). Different scales.

$T$	temperature	$Ri$	(bulk) Richardson number
$H_2O$	water (vapor)	$\Omega$	decoupling metric
$CO_2$	carbon dioxide	$\zeta$	stability parameter
$CH_4$	methane	TKE	turbulent kinetic energy
SW	shortwave radiation	$u_*$	friction velocity
LW	longwave radiation	$\sigma_x$	turbulence intensity of $x$
SH	sensible heat flux	$\frac{w'x'}{w'x'}$	vertical flux of $x$
LH	latent heat flux	$y_B$	anisotropy
R	radiation balance		
SEB	surface energy balance		

Table 3.1: Used symbols.

quality flagging (e.g. `flag_stationarity()`, `flag_distortion()`) and initially accumulated to averaging times of 1 and 30 minutes (`accumulate_timeseries()`). The flux footprint climatologies shown in Fig. 3.1 are calculated with the function `calc_flux_footprint_climatology(..., method = "KM2001")`, here exemplarily with the Kormann and Meixner (2001)-model, and geo-localized (`locate_flux_footprint()`), and indicate valley-following flow channeling at Finse and a lake-dominated fetch at Langtjern.

### 3.1 Example 1: Finse

Fig. 3.2 shows timeseries of a two-day case study during cold conditions at Finse (17.03.-18.03.2018) generated by 'Reddy'. From the post-processed eddy-covariance data several diagnostics (e.g. `calc_Ri()`, `calc_decoupling_metric()`, `calc_tke()`, `calc_anisotropy()`) as well as the surface energy balance (`plot_seb()`) were calculated and visualized. These two clear-sky days are characterized by a pronounced diurnal cycle and strongly stable stratification during the calm night with Richardson numbers exceeding

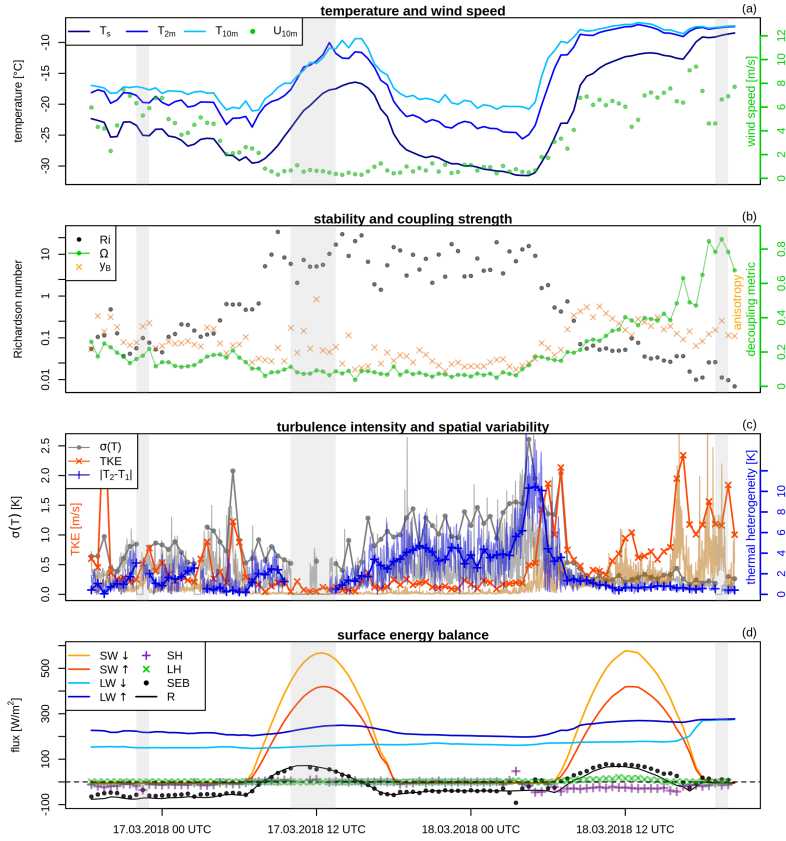


Figure 3.2: Case study from Finse, 17.03.2018-18.03.2018: (a) Temperature and wind speed, (b) Richardson number and decoupling metric (based on vertical gradients between atmosphere and surface) and anisotropy, (c) turbulence intensity and thermal heterogeneity (30 minutes and 1 minute averaging), (d) surface energy balance. Shaded areas mark bad quality flags (QC = 2).

$Ri > 10$ . While during daytime the atmosphere is well-mixed with similar temperatures at 2 m and 10 m (Fig. 3.2a), surface and atmosphere appear decoupled throughout the entire day (Fig. 3.2a, b). At the same time, anisotropy, turbulent potential energy and the temperature difference between the two sites are enhanced (Fig. 3.2c). The surface energy balance (Fig. 3.2d) is dominated by the strong radiative fluxes, with radiative cooling during nighttime and warming during daytime (likely transferred to snow-melt), while the turbulent fluxes (amplitude smaller than  $20 \text{ W/m}^2$ ) and the ground heat flux ( $< 2 \text{ W/m}^2$ , not shown) cannot close the surface energy balance, leading to an average unclosure of  $-11.3 \text{ W/m}^2$  and an unclosure ratio of 10.8 % for these two days.

The analysis indicates strong variability in near-surface temperature profiles, and a relation between enhanced spatial thermal heterogeneity and strongly stable stratification, which can be further interpreted by relating physical to information decoupling (Mack et al., 2025a).

### 3.2 Example 2: Langtjern

Fig. 3.3 shows the composite MRDs and ogives during ice-covered and ice-free period at lake Langtjern. The MRDs are calculated and visualized with the functions `calc_mrd()`, `plot_mrd()`, from which a suggestion for the averaging time is derived (`suggest_averaging_time()`) and the ogives as integrated co-spectrum are calculated (`calc_ogive()`, `plot_ogive()`). The transition between ice-covered and ice-free period results in increasing water vapor concentrations and increasingly positive latent heat flux, while at the

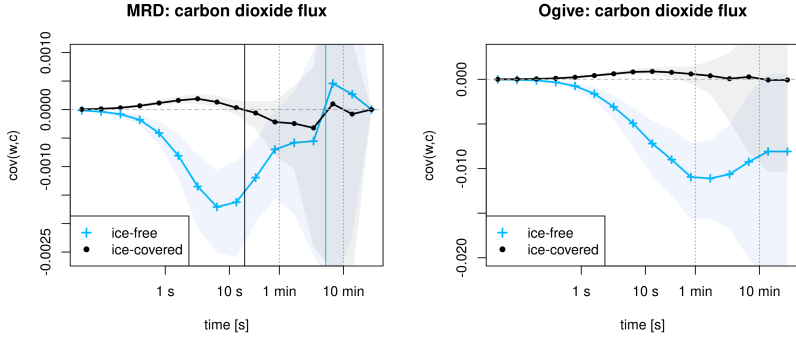


Figure 3.3: Composite MRDs and ogives during ice-covered and ice-free period at lake Langtjern. The shaded areas mark the inter-quartile-range and the solid vertical line the suggested averaging time.

same time the CO<sub>2</sub> concentration decreases and the CO<sub>2</sub> flux becomes negative (CO<sub>2</sub> uptake). Thereby, the spectral analysis of the CO<sub>2</sub> flux shows significant contributions from low-frequency submeso-scale motions, which are even of the opposite sign than the high-frequency turbulent motions. Particularly during the low-flux ice-covered period, the 30 minutes block averaging would lead to a cancellation of the high- and low-frequency contributions, going along with a slow convergence rate of the ogive. While the ogive analysis would suggest to use even longer averaging periods for wintertime stable conditions to reach stationarity, a meteorological study of intermittent trace gas transport could consider using smaller block averaging corresponding to the identified co-spectral gap following the Vickers and Mahrt (2003)-algorithm (here: ice-covered 30 s, ice-free 5 min).

This example illustrates the intrigue of choosing a suitable averaging time, which has a decisive impact on the overall flux and thus also on the budgets of evaporation and net ecosystem exchange. With 'Reddy', it is easily possible to start with a standard post-processing routine to get an overview of the meteorological and environmental conditions, and then use spectral analysis to reconsider the chosen averaging time to account for changing surface and environmental conditions.

### 3.3 Example 3: Iškoras

For the permafrost peatland site Iškoras, we fit the flux-variance relations for scalar concentrations using 'Reddy' (Fig. 3.4). For this,  $\Phi_x := \sigma_x / x_*$  with  $x_* = \overline{w'x'}/u_*$  is calculated using the function `calc_phix()` and a linear regression of the form  $\Phi_x = C_x \cdot |\zeta|^{-1/3}$  according to Katul et al. (1994) is performed, resulting in the scaling constants  $C_{\text{H}_2\text{O}} = 1.209 (R^2 = 0.85)$  for latent heat flux and  $C_{\text{CO}_2} = 1.248 (R^2 = 0.87)$  for CO<sub>2</sub> flux, while the flux-variance relation for methane  $C_{\text{CH}_4} = 1.540 (R^2 = 0.79)$  is associated with larger spread (not shown). For observational setups where only the variance is known or for validating the fitted flux-variance relations, the function `scale_phic()` (and the equivalents `scale_T()`, `scale_u()`, `scale_w()` for temperature, horizontal and vertical wind) can be used to estimate the respective fluxes. Validating the estimated fluxes using the fitted flux-variance relations compared to the measured fluxes, reveals correlations of 0.91 for H<sub>2</sub>O, 0.51 for CO<sub>2</sub> and 0.14 for CH<sub>4</sub>. The lower correlations for CO<sub>2</sub> and CH<sub>4</sub> are related to their heterogeneous source distribution contradicting assumptions of Monin-Obukhov similarity theory (e.g. Hsieh et al., 2008). Disaggregating the flux contributions of different surface types (here: palsa, mire, pond) (Pirk et al., 2024), could be a way to improve flux-variance relations per surface type. This once again

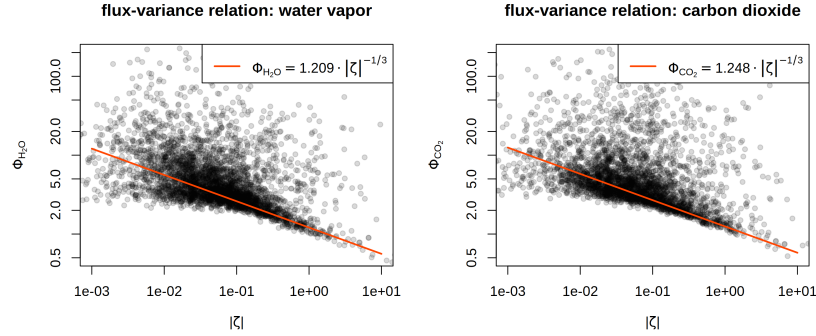


Figure 3.4: Flux-variance relations for water vapor and carbon dioxide fitted based on two years (2020-2021) of eddy-covariance measurements at Iškoras.

highlights the difficulty of modelling turbulent trace gas fluxes in complex environments and also shows that quality flags (such as the integral turbulence characteristic flag), which reject measurements that do not match literature-based flux-variance relations, should be used with caution.

### 3.4 Further Applications

Due to the modular structure of the 'Reddy'-package, it enables several applications ranging from quick in-field real-time post-processing of measurement data to station management and detailed scientific investigations. To allow a quick introduction to the package and standard analysis procedures of eddy-covariance measurements, the following jupyter notebooks (available at [https://noctiluc3nt.github.io/ec\\_analyze/](https://noctiluc3nt.github.io/ec_analyze/)) have been compiled covering the topics:

- (1) Post-processing
- (2) Basic turbulence diagnostics
- (3) Quadrant analysis
- (4) Spectral analysis
- (5) Flux footprint estimation
- (6) Invariant analysis of Reynolds stress tensor
- (7) Surface energy balance
- (8) Turbulence parameterizations in numerical weather prediction and climate models

This low-threshold introduction is aimed at new users of eddy-covariance data and was used at the University of Oslo as part of teaching on eddy-covariance data analysis as tool in boundary-layer meteorology in connection with a field excursion. Ready-made evaluation tools and functions enable rapid learning progress and at the same time give interested students the opportunity to engage with the source code, so that eddy-covariance data analysis is not treated as a black box.

## 4 Discussion

The open-source package 'Reddy' provides a framework for reproducible post-processing and analysis of eddy-covariance data. It has been successfully applied in scientific studies, for near real-time station monitoring and in teaching. The user can choose from a pool of modular-built functions and combine them in the most appropriate way in their customized workflow, for their specific site and field of application, including meteorology, hydrology and ecology. 'Reddy' thus enables a broad range of applications beyond standard turbulent surface flux calculations, e.g. investigating lateral fluxes and intermittency in winter-time turbulence in complex heterogeneous environments. At the same time, it requires the user to have a fundamental understanding of eddy-covariance data analysis, for which a hands-on introduction with jupyter notebooks covering the most important data analysis steps is provided. The 'Reddy' package and its focus on turbulence in heterogeneous environments serves as supplement to other open-source packages for eddy-covariance data processing (e.g. Metzger et al., 2017; Volk et al., 2021), and packages dealing with different application areas, e.g. 'REddyProc' focusing on gap-filling and flux partitioning (Wutzler et al., 2018) or 'bigleaf' for deriving physiological ecosystem properties from eddy-covariance measurements (Knauer et al., 2018). The package has been originally developed in the language R, but a similar version for Python ('Reddy4py') is openly available. The 'Reddy' package is maintained on GitHub, and creating issues or extensions is absolutely welcomed.

## 5 Conclusion

We introduced the open-source software package 'Reddy', which serves as toolbox for eddy-covariance data processing and analysis, accompanied by a detailed documentation and a set of jupyter notebooks introducing new users to eddy-covariance data analysis. We showcased the applicability of 'Reddy' by analyzing a case study of stable boundary layer dynamics at an alpine tundra site, for spectral analysis during ice-cover transition at a boreal lake and for fitting flux-variance relations at a permafrost peatland.

## Code and Data Availability

The 'Reddy' package is available on GitHub (<https://github.com/noctiluc3nt/Reddy>) accompanied by a manual and a hands-on introduction to eddy-covariance data analysis ([https://noctiluc3nt.github.io/ec\\_analyze/](https://noctiluc3nt.github.io/ec_analyze/)). The used terrain data provided by Kartverket is available at <https://www.geonorge.no/>.

## Acknowledgements

The R core team (R Core Team, 2024) is acknowledged. This work was supported by the European Research Council (project #101116083) and is a contribution to the strategic research initiative LATICE (Faculty of Mathematics and Natural Sciences, University of Oslo, project #UiO/GEO103920).

## References

Aubinet, M., Vesala, T., and Papale, D. (2012). Eddy Covariance. A Practical Guide to Measurement and Data Analysis. *Springer*.

Baldocchi, D. D. (2003). Assessing the eddy covariance technique for evaluating carbon dioxide exchange rates of ecosystems: past, present and future. *Global Change Biology*.

Baldocchi, D. D. (2020). How eddy covariance flux measurements have contributed to our understanding of Global Change Biology. *Global Change Biology*, 26:242–260.

Banerjee, S., Krahl, R., Durst, F., and Zenger, C. (2007). Presentation of anisotropy properties of turbulence, invariants versus eigenvalue approaches. *Journal of Turbulence*, 8(N32).

Charnock, H. (1955). Wind stress on a water surface. *Q J R Meteorol soc*, 81:639–640.

Clayer, F., Thrane, J.-E., Brandt, U., Dörsch, P., and de Wit, H. (2021). Boreal Headwater Catchment as Hot Spot of Carbon Processing From Headwater to Fjord. *Journal of Geophysical Research: Biogeosciences*, 126(e2021JG006359).

de Wit, H. A., Clayer, F., and Kaste, Ø. Norling, M. (2024). From anthropogenic toward natural acidification: Effects of future deposition and climate on recovery in a humic catchment in Norway. *Ecological Research*, 40:352–364.

Eddelbuettel, D. (2013). *Seamless R and C++ Integration with Rcpp*. Springer. Use R!

Foken, T. and Wichura, B. (1996). Tools for quality assessment of surface-based flux measurements. *Agricultural and Forest Meteorology*, 78(1-2):83–105.

Fratini, G. and Mauder, M. (2014). Towards a consistent eddy-covariance processing: an intercomparison of EddyPro and TK3. *Atmos Meas Tech*, 7:2273–2281.

Ganapathisubramani, B., Hutchins, N., Hambleton, W. T., Longmire, E. K., and Marusic, I. (2005). Investigation of large-scale coherence in a turbulent boundary layer using two-point correlations. *J. Fluid Mech.*, 254:57–80.

Hsieh, C.-I., Lai, M.-C., Hsia, Y.-J., and Chang, T.-J. (2008). Estimation of sensible heat, water vapor, and CO<sub>2</sub> fluxes using the flux-variance method. *Int J Biometeorol*, 52:521–533.

Ibrom, A., Dellwik, E., Larsen, S. E., and Pilegaard, K. (2007). On the use of the Webb–Pearman–Leuning theory for closed-path eddy correlation measurements. *Tellus B: Chemical and Physical Meteorology*, 59(5):937–946.

Katul, G., Goltz, S. M., Hsieh, C.-I., Cheng, Y., Mowry, F., and Sigmund, J. (1994). Estimation of surface heat and momentum fluxes using the flux-variance method above uniform and non-uniform terrain. *Boundary-Layer Meteorology*, 74:237–260.

Kljun, N., Calanca, P., Rotach, M. W., and Schmid, H. P. (2015). A simple two-dimensional parameterisation for Flux Footprint Prediction (FFP). *Geoscientific Model Development*, 8:3695–3713.

Knauer, J., El-Madany, T. S., Zaehle, S., and Migliavacca, M. (2018). Bigleaf – An R package for the calculation of physical and physiological ecosystem properties from eddy covariance data. *PLOS One*, 13(8).

Kormann, R. and Meixner, F. X. (2001). An analytical footprint model for non-neutral stratification. *Boundary-Layer Meteorology*, 99:207–224.

Lehner, M., Rotach, M. W., and Obleitner, F. (2019). A Method to Identify Synoptically Undisturbed, Clear-Sky Conditions for Valley-Wind Analysis. *Boundary-Layer Meteorology*, 173:435–450.

LI-COR Biosciences (2017). *EddyPro Software. Instruction Manual*.

Liu, H., Peters, G., and Foken, T. (2001). New equations for sonic temperature variance and buoyancy heat flux with an omnidirectional sonic anemometer. *Boundary-Layer Meteorol*, 100:459–468.

Mack, L., Berntsen, T. K., Vercauteren, N., and Pirk, N. (2024). Transfer Efficiency and Organization in Turbulent Transport over Alpine Tundra. *Boundary-Layer Meteorology*, 190(38).

Mack, L., Kähnert, M., and Pirk, N. (2025a). Probabilistic modelling of atmosphere-surface coupling with a copula Bayesian network. *arXiv[physics.ao-ph]*.

Mack, L., Kähnert, M., Rauschenbach, Q., Frank, L., Hasenburg, F. H., Huss, J.-M., Jonassen, M. O., Malpas, M., Batrak, Y., Remes, T., Pirk, N., and Thomas, C. K. (2025b). Stable Boundary Layers in an Arctic Fjord-Valley System: Evaluation of Temperature Profiles Observed From Fiber-Optic Distributed Sensing and Comparison to Numerical Weather Prediction Systems at Different Resolutions. *Journal of Geophysical Research: Atmospheres*, 130(e2024JD042825).

Mahrt, L. (1998). Nocturnal Boundary-Layer Regimes. *Boundary-Layer Meteorology*, 88:255–278.

Mahrt, L. (2011). The Near-Calm Stable Boundary Layer. *Boundary-Layer Meteorology*, 140:343–360.

Mahrt, L. (2014). Stably Stratified Atmospheric Boundary Layers. *Annu. Rev. Fluid Mech*, 46:23–45.

Mammarella, I., Peltola, O., Nordbo, A., Järvi, L., and Rannik, Ü. (2016). Quantifying the uncertainty of eddy covariance fluxes due to the use of different software packages and combinations of processing steps in two contrasting ecosystems. *Atmos Meas Tech*, 9:4915–4933.

Marty, C. and Philipona, R. (2000). The clear-sky index to separate clear-sky from cloudy-sky situations in climate research. *Geophysical Research Letters*, 27:2649–2652.

Massmann, W. J. (2000). A simple method for estimating frequency response corrections for eddy covariance systems. *Agricultural and Forest Meteorology*, 104:185–198.

Mauder, M., Cuntz, M., Drüe, C., Graf, A., Rebmann, C., Schmid, H. P., Schmidt, M., and Steinbrecher, R. (2013). A strategy for quality and uncertainty assessment of long-term eddy-covariance measurements. *Agricultural and Forest Meteorology*, 169:122–135.

Mauder, M., Foken, T., Clement, R., Elbers, J. A., Eugster, W., Grünwald, T., Heusinkveld, B., and Kolle, O. (2008). Quality control of CarboEurope flux data – Part 2: Inter-comparison of eddy-covariance software. *Biogeosciences*, 5:451–562.

Metzger, S., Durden, D., Sturtevant, C., Luo, H., Pingintha-Durden, N., Sachs, T., Serafimovich, A., Hartmann, J., Li, J., Xu, K., and Desai, A. R. (2017). eddy4R 0.2.0: a DevOps model for community-extensible processing and analysis of eddy-covariance data based on R, Git, Docker, and HDF5. *Geoscientific Model Development*, 10:3189–3206.

Moncrieff, J., Clement, R., Finnigan, J., and Meyers, T. (2005). Averaging, Detrending and Filtering of Eddy Covariacne Time Series. *in: Handbook of Micrometeorology*, Kluwer Academic Publishers.

Neftel, A., Spirig, C., and Ammann, C. (2008). Application and test of a simple tool for operational footprint evaluations. *Environmental Pollution*, 152:644–652.

Nieuwstadt, F. T. M. (1981). The Steady-state Height and Resistance Laws of the Nocturnal Boundary Layer: Theory Compared with Cabauw Observations. *Boundary-Layer Meteorology*, 20:3–17.

Ozmidov, R. V. (1965). On the turbulent exchange in a stably stratified ocean. *Izv. Acad. Sci. USSR Atmos. Oceanic Phys*, 1:861–871.

Panofsky, H. and Dutton, J. (1984). Atmospheric Turbulence: Models and Methods for Engineering Applications. *John Wiley and Sons*.

Pastorello, G., Trotta, A., Canfora, E., et al. (2020). The FLUXNET2015 dataset and the ONEFlux processing pipeline for eddy covariance data. *Scientific Data*, 7(225).

Peltola, O., Aslan, T., Ibrom, A., NEmitz, E., Rannik, Ü., and Mammarella, I. (2021a). The high-frequency response correction of eddy covariance fluxes – Part 1: An experimental approach and its interdependence with the time-lag estimation. *Atmos Meas Tech*, 14:5071–5088.

Peltola, O., Lapo, K., and Thomas, C. K. (2021b). A Physics-Based Universal Indicator for Vertical Decoupling and Mixing Across Canopies Architectures and Dynamic Stabilities. *Geophysical Research Letters*, 48(e2020GL091615).

Pirk, N., Aalstad, K., Mannerfelt, E. S., Clayer, F., de Wit, H., Christiansen, C. T., Althuizen, I., Lee, H., and Westermann, S. (2024). Disaggregating the Carbon Exchange of Degrading Permafrost Peatlands Using Bayesian Deep Learning. *Geophysical Research Letters*, 51(e2024GL109283).

Pirk, N., Aalstad, K., Yilmaz, Y. A., Vatne, A., Popp, A. L., Horvath, P., Bryn, A., Vollnes, A. V., Westermann, S., Berntsen, T. K., Stordal, F., and Tallaksen, L. M. (2023). Snow-Vegetation-Atmosphere Interactions in Alpine Tundra. *Biogeosciences*, 20:2031–2047.

Pirk, N., Sievers, J., Mertes, J., Parmentier, F.-J. W., Mastepanov, M., and R., C. T. (2017). Spatial variability of CO<sub>2</sub> uptake in polygonal tundra: assessing low-frequency disturbances in eddy covariance flux estimates. *Biogeosciences*, 14:3157–3169.

R Core Team (2024). *R: A Language and Environment for Statistical Computing*. R Foundation for Statistical Computing, Vienna, Austria.

Rotach, M. W. and Holtslag, A. A. M. (2025). Ideal and Real Atmospheric Boundary Layers. *Elsevier Academic Press*.

Schotanus, P., Nieuwstadt, F. T. M., and De Bruin, H. A. R. (1983). Temperature measurement with a sonic anemometer and its application to heat and moisture fluxes. *Boundary-Layer Meteorology*, 26:81–93.

Shaw, R. H., Tavanger, J., and Ward, D. P. (1983). Structure of the Reynolds stress in a Canopy layer. *J Clim Appl Meteorol*, 22:1922–1931.

Sievers, J., Papakyriakou, T., Larsen, S. E., Jammet, M. M., Rysgaard, S., Sejr, M. K., and Sørensen, L. L. (2015). Estimating surface fluxes using eddy covariance and numerical ogive optimization. *Atmos. Chem. Phys.*, 15:2081–2103.

Stiperski, I. and Calaf, M. (2018). Dependence of near-surface similarity scaling on the anisotropy of atmospheric turbulence. *Q J R Meteorol Soc*, 144:641–657.

Stoy, P., Mauder, M., and Foken, T. (2013). A data-driven analysis of energy balance closure across FLUXNET research sites: the role of landscape scale heterogeneity. *Agric For Meteorol*, 171:137–152.

van de Water, W. and Herweijer, J. A. (1999). High-order structure functions of turbulence. *J. Fluid Mech.*, 387:3–37.

Vickers, D. and Mahrt, L. (2003). The Cospectral Gap and Turbulent Flux Calculations. *Journal of Atmospheric and Oceanic Technology*, 20:660–672.

Volk, J., Huntington, J., Allen, R., Melton, F., Anderson, M., and Kilic, A. (2021). flux-data-qaqc: A Python Package for Energy Balance Closure and Post-Processing of Eddy Flux Data. *Journal of Open Source Software*, 6(66).

Webb, E. K., Pearman, G. I., and Leuning, R. (1980). Correction of flux measurements for density effects due to heat and water vapour transfer. *Q J R Meteorol Soc*, 106(447):85–100.

Wilczak, J. M., Oncley, S. P., and Stage, S. A. (2001). Sonic anemometer tilt correction algorithms. *Boundary-Layer Meteorology*, 99:127–150.

Winstral, A., Jonas, T., and Helbig, N. (2017). Statistical Downscaling of Gridded Wind Speed Data Using Local Topography. *Journal of Hydrometeorology*, 18:335–348.

Wutzler, T., Lucas-Moffat, A., Migliavacca, M., Knauer, J., Sickel, K., Sigut, L., Menzer, O., and Reichstein, M. (2018). Basic and extensible post-processing of eddy covariance flux data with REddyProc. *Biogeosciences*, 15:5015–5030.